# Sensitivity of Glaze Ice Accretion and Iced Aerodynamics Prediction to Roughness

Alexandros Kontogiannis[1], Aviral Prakash[1], Eric Laurendeau[1] and Frédéric Moens[2]

[1] *Department of Mechanical Engineering, Polytechnique Montreal,*
*2900 Edouard Montpetit Blvd, Montreal, QC, H3T 1J4, Canada*
[2] *ONERA, The French Aerospace Lab, 92190 Meudon, France*

Email: *alexandros.kontogiannis@polymtl.ca*

## ABSTRACT

A study of the effect of the assumed ice roughness on ice shape prediction and aerodynamic performance degradation has been conducted to quantify the sensitivity of glaze ice accretion prediction according to the value of equivalent sand grain roughness height ($k_s$). The motivation stems from the fact that a good representative value of $k_s$ is almost never known *a priori*, and usually crude roughness models are employed. First, a validation of the icing suite NSCODE-ICE is presented, for both ice-accretion and aerodynamic performance degradation, using three icing experiments performed in the Icing Research Tunnel (IRT) of NASA. Then, a sensitivity study is conducted for a range of $k_s$ values that are most common for ice formation on transport aircraft wings, encountering atmospheric icing conditions. The goal is to quantify the variation of aerodynamic performance loss due to the uncertainty introduced by the choice of the $k_s$ value.

## NOMENCLATURE

| | |
|---|---|
| $c$ | airfoil chord length [m] |
| $h_c$ | convective heat transfer coeff. [Wm$^{-2}$K$^{-1}$] |
| $k$ | true roughness height [m] |
| $k_s$ | equivalent sand grain roughness heigh [m] |
| $Pr_t$ | turbulent Prandlt number |
| $S_{corr}$ | rough-to-smooth wall surface area ratio |
| $T_s$ | static air temperature [K] |
| $V_\infty$ | freestream velocity [m s$^{-1}$] |
| APD | Aerodynamic Performance Degradation |
| DERM | Discrete Element Roughness Method |
| IRT | Icing Research Tunnel (NASA Glenn) |
| LWC | Liquid Water Content [g/m$^3$] |
| MVD | Mean Volume Diameter [$\mu$m] |

## 1 INTRODUCTION

Accurate prediction of ice accretion and subsequent aerodynamic performance degradation (APD) is of major importance for the design and certification of civil transport aircrafts that imposes constraints in every design phase [15]. The current goal in this field of research is to close the gap between the natural in-flight icing, the icing wind tunnel test results, and the prediction via numerical simulation. In order to achieve this, the icing simulation methods should be mature enough, incorporating physical models that can be well calibrated with existing experimental icing databases, if they are to be used for the design of the current, as well as the next generation of aircrafts.

For atmospheric and flight conditions that favor glaze ice accretion, the physical phenomena that take place are usually highly complicated, stochastic (followed by poor experimental repeatability), and not adequately modeled by the state-of-the-art computational icing simulations. Because of this, the predictive confidence [29] in glaze ice conditions is much less than that of rime ice conditions, while also the aerodynamic performance degradation is more severe due to glaze ice accretion. Although, natural (aleatoric) as well as computational modeling (epistemic) uncertainties dominate glaze ice prediction, the latter is usually approached in a deterministic way by decoupling the multiphysical process and following a sequential approach to predict the flow field and the convective heat transfer at the wall, the collection efficiency by computing the droplet trajectories, and the ice mass accretion by a means of a thermodynamic model. Other, non-deterministic modeling approaches for icing accretion exist [27][8], but they are rarely used as they are not mature yet. Many aleatoric and epistemic uncertainties in an icing simulation are

Table 1: Icing conditions for ice shape prediction and APD benchmark of icing suites. [28]

| Condition No. | Airfoil | Chord m | Airspeed m/s | AoA deg. | MVD μm | LWC $g/m^3$ | Total Temp. $^oC$ | Static Temp. $^oC$ | Spray Time s |
|---|---|---|---|---|---|---|---|---|---|
| 3 | NACA0012 | 0.5334 | 102.9 | 4 | 30 | 1.80 | -5.6 | -10.9 | 360 |
| 7 | GLC305 | 0.3048 | 139.4 | 0 | 19 | 1.12 | -7.9 | -17.6 | 138 |
| 9 | GLC305 | 0.6096 | 89.4 | 0 | 35 | 1.30 | -6.0 | -10.0 | 360 |

related to ice roughness because it can vary according to the atmospheric and flight conditions and because its effects on convective heat transfer, which governs the ice accretion phase, are not well understood. Convective heat transfer through rough surfaces can be numerically simulated using one of the three following approaches: i) mesh-resolved roughness, ii) discrete element roughness method (DERM) and iii) use of equivalent sand grain roughness height ($k_s$) corrections. Solving RANS equations to roughness length scales [6] is computationally expensive and is not often used for industrial applications. Discrete element roughness method, introduced by Schlichting [23], and further formulated for academic roughness in [10] and extended for random roughness in [19], takes into account the effect of roughness by modifying the boundary layer equations to account for the flow blockage due to the local roughness geometry and by using additional correcting source terms to the momentum and the energy equations. However, since the modifications introduced in RANS-based equations using DERM come at a considerable cost of implementation, this method is not usually preferred. Therefore, RANS-based as well as potential flow icing simulation methods, generally rely on momentum and thermal corrections [16] based on the equivalent sand grain roughness height empirical model, proposed by Schlichting [23] (later revised by Coleman [9]) and constructed upon experimental data of Nikuradse [21]. One of the main drawbacks of this method, is that there is no common consensus, at least in the field of icing, on how to define the $k_s$ value of a random ice roughness. Correlations that utilize several geometric metrics of the true roughness to estimate an equivalent $k_s$ value exist [11] [25], but the true ice roughness is not known *a priori* when an icing simulation is performed. Again, these correlations have been found to incorporate a high degree of uncertainty [4]. Another issue that arises with the use of $k_s$ based corrections, is that the $k_s$ empirical model was devised to correct for skin friction and not for heat transfer. There is an inherent incompatibility in the model to be capable of providing a satisfactory prediction of both skin friction and convective heat transfer [5] [2] because

Reynold's analogy is violated for rough surfaces.

As the ice shape prediction for glaze ice depends significantly on the estimated convective heat transfer coefficient [12] which, in turn, depends considerably on the roughness parameters, there is a need for a dedicated study to analyze the effect of assumed ice roughness on ice shape prediction and the subsequent aerodynamic performance degradation. Effects of equivalent sand grain roughness ($k_s$) on ice shape prediction have been highlighted by other authors [3] [13], however limited glaze ice test cases were selected and the effect on glaze shape characteristics like horn angle, horn height and ice limits were not quantified. In this study, the strong effect of roughness on ice shape prediction and APD is presented for glaze ice shapes that were simulated with NSCODE-ICE and compared with experimental shapes obtained in the Icing Research Tunnel of NASA [31].

## 2 NUMERICAL ICING SIMULATION

The icing simulation framework used in this study is the in-house code NSCODE-ICE developed at Polytechnique Montreal. It is a multi-layer structured RANS-based ice accretion code suited for both ice shape prediction and aerodynamic performance degradation analysis for purely 2D as well as 2D infinite-swept flows (2.5D) [17]. The framework consists of the following modules

- Structured, cell-centered, compressible Navier-Stokes code (NSCODE) for the flowfield [22]

- Eulerian droplet solver for water impingement and collection efficiency estimation [17]

- Thermodynamic ice-accretion model for ice-growth computation, including local shear stress effect on water runback [18]

- Algebraic node based or level-set B-spline based geometric evolution of accreted ice [7]

- Automatic iced-airfoil grid generation at each layer using NSGRID [14]

The flow and droplet solver are used with a second order matrix based dissipation scheme (MATD) [26], three levels of multigrid (W-type) and a LU-SGS solver. The selected turbulence model is the one-equation model of Spalart-Allmaras (S-A), with the Boeing extension [2] to account for wall roughness by modifying the distance to the nearest wall $d$ (used in S-A model) by a length proportional to $k_s$. The iterative Messinger model [32] is used for ice accretion and the convective heat transfer coefficient $h_c$ is computed using the method proposed by ONERA [20], which requires two flow computations for each time-step (or ice-layer). The equivalent-sand grain roughness height $k_s$ can be either given as input to the code or computed from the given icing and flight conditions using an empirical formula of the form [24]

$$k_s = \mathcal{F}(LWC, MVD, T_s, V_\infty, c) \qquad (1)$$

which was used in previous versions of NASA's icing accretion code LEWICE.

## 3 NASA/ONERA BENCHMARK

The glaze ice prediction benchmark initiated by NASA [31] and also performed by ONERA [28], for 14 extreme icing conditions, is also performed for NSCODE-ICE for both ice accretion prediction and aerodynamic performance degradation.

### 3.1 Ice Shape Prediction

The ice shape prediction capability of NSCODE-ICE was tested against LEWICE (NASA), IGLOO2D (ONERA) and experimental results from IRT. The icing conditions for the cases under study are taken from [31][28] and summarized in Table 1. The comparison of the three icing suites is presented in Figure 1 where IGLOO2D-MS(50) stands for IGLOO2D with a multistep method of 50 steps, and equivalently, NSCODE-ICE MS(20) for 20 steps. It is observed that, regarding the horn angles and heights, NSCODE-ICE compares well with the experimental results. An overestimation of horn angle and height in Figure 1b by IGLOO2D is due to an overestimation of the convective heat transfer, probably due to selection of higher value of the ice roughness. In terms of the ice limits, IGLOO2D and NSCODE-ICE overestimate both upper and lower icing limits mainly for Condition 3 (Figure 1a). The greater overestimation of IGLOO2D is due to the use
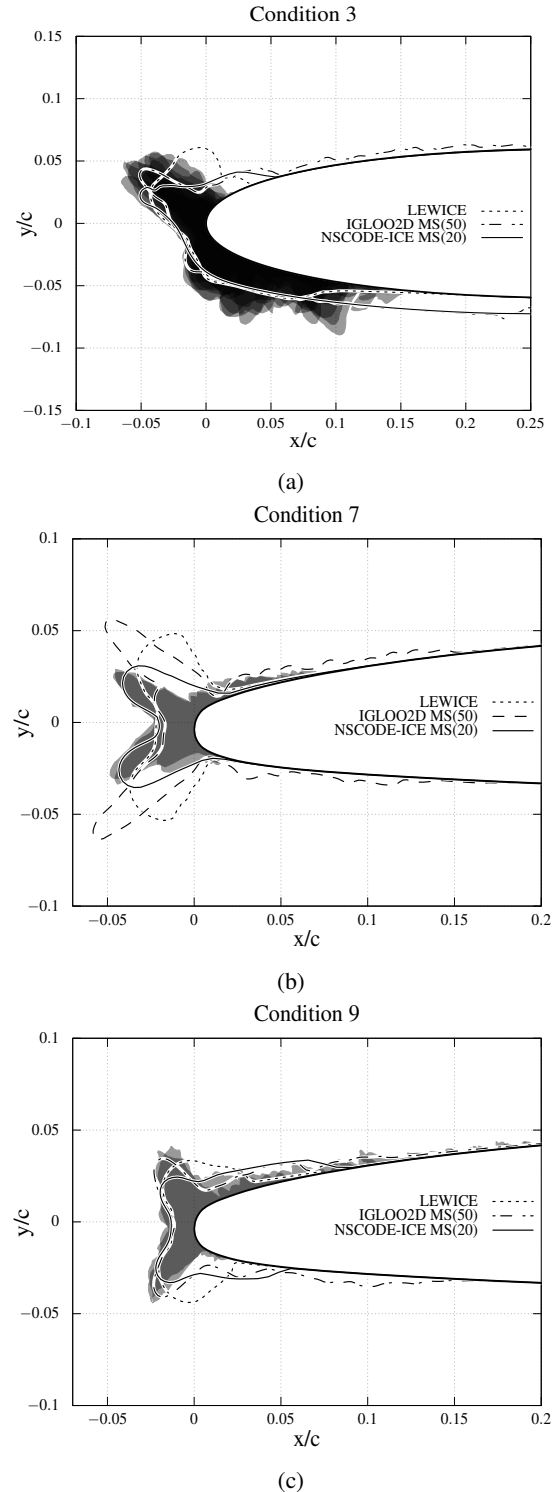


(a)



(b)



(c)

Figure 1: Ice shape prediction comparing to experimental (grayscale solids) for LEWICE, IGLOO2D [28] and NSCODE-ICE. For NSCODE-ICE, $k_s$ is taken as 0.33mm, 0.16mm and 0.37mm for conditions 3, 7 and 9 respectively.

of the classical Messinger ice accretion model [28], which does not incorporate skin friction and pressure forces to drive the water film. Instead, NSCODE-ICE uses an iterative Messinger model [32], which incorporates the skin friction forces on the water film. Nevertheless, despite the accretion model used, an overestimation of the icing limits can also occur if the local heat transfer is underpredicted because of selection of lower value of ice roughness. Both IGLOO2D and NSCODE-ICE use a constant value of ice roughness throughout the airfoil surface, while LEWICE has also a variable roughness option [30]. All three icing suites agree remarkably well regarding the ice thickness at the stagnation point for the cases under study. The geometric characteristics of the these ice shapes (Figure 1) are quantified as in [28] and presented in Table 4.

## 3.2 APD Prediction

NSCODE-ICE, being a RANS-based icing code, is also capable of estimating the degradation in aerodynamic performance as a result of the deposited ice on the airfoil. Initially, the APD due to the real ice shape (obtained in IRT) of Condition 7 [28] was assessed using NSCODE. To properly resolve the iced surface details, a mesh of 450k cells was generated with NS-GRID, having a maximum $y^+$ value of 0.3. The airfoil surface is considered partially rough, i.e. roughness corrections imposed by the extended S-A turbulence model [2] are taken into account only for the iced surface. The numerical schemes used were already mentioned in Section 2. All results are converged to a scaled density residual of $O(10^{-5})$ and the convergence curves are presented in Figure 2b for different angles of attack. The predicted performance degradation due to the real ice shape (NSCODE-IRT) with NSCODE is compared with FUN3D results [31] in Figure 2c. The lift and drag is predicted very well for angles ranging from -4 to 4 and at 6 degrees a strong deviation is observed which is accompanied by a significant region of separated, recirculatory flow aft of the upper horn (Figure 2a). The APD is also evaluated for the predicted ice shape with NSCODE-ICE (using NSCODE) and the predicted ice shape of LEWICE (Figure 1b), computed with NASA's FUN3D solver.

## 4 ROUGHNESS SENSITIVITY

## 4.1 Sensitivity on Ice Shape

Parametric study of the evolution of ice shape according to $k_s$ is performed to indicate the extent to which
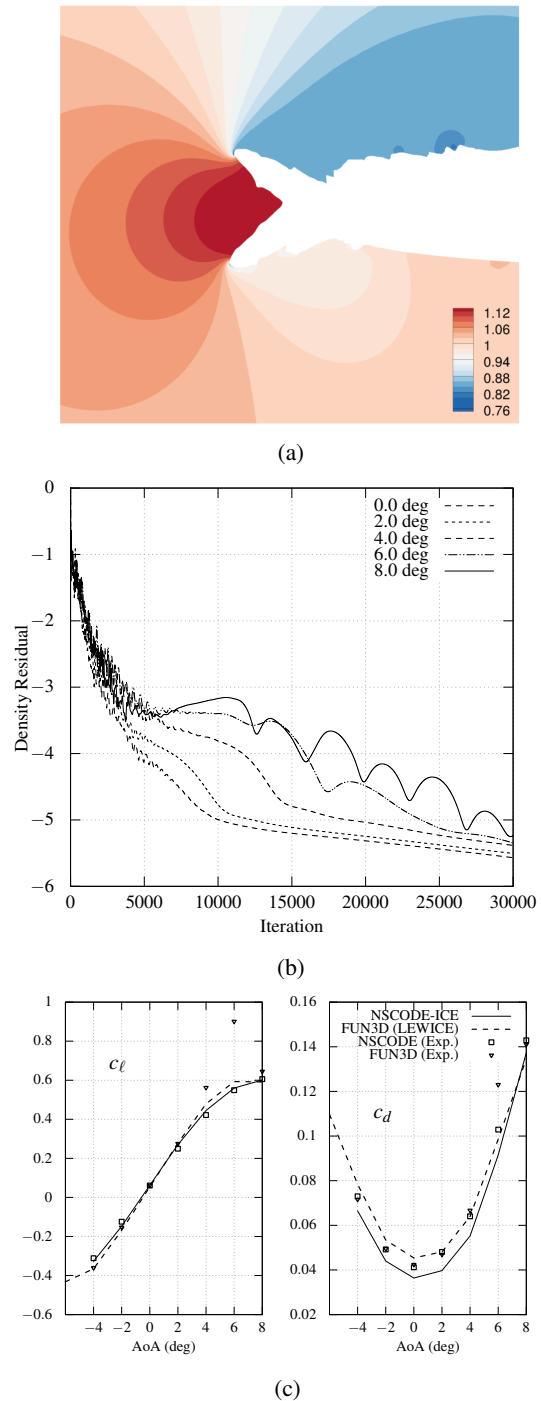


(a)



(b)



(c)

Figure 2: a) Pressure contours at 4 deg. (NSCODE (Exp.)), b) convergence of NSCODE (Exp.) at different AoA and c) computation of degraded aerodynamic performance for computed ice shape (NSCODE-ICE) and real ice shape (NSCODE (Exp.)) and comparison with NASA (FUN3D) results and LEWICE.

$k_s$ affects the predicted ice shape. In Figure 3, it is observed that $k_s$ has considerable effect on the determination of different ice shape metrics like upper/lower horn angle and horn height as well as ice limits. In all the cases, the ice limits extend far aft the leading edge for low $k_s$ values and decrease in length for high values $k_s$. This is because lower $k_s$ leads to lower convective heat transfer coefficient ($h_c$) which increases the runback water letting it freeze at a larger chordwise distance.

The value of $k_s$ also affects the horn angle and the horn height. As the ice builds up over several layers in a multi-step simulation, ice shape prediction at the previous layer determines the direction of propagation of horn height. As the value of $k_s$ affects the predicted ice shape at each layer, the horn angle also changes. This effect is more prominent for Condition 7 (Figure 3b). The ice horns generally grow along the direction of maximum $h_c$. For Condition 3 (Figure 3a) and 9 (Figure 3c), there is no significant effect of $k_s$ on horn angle since the direction of ice growth does not change considerably with the evolving ice. The increase in $h_c$ with $k_s$ also leads to an increase in the horn height. Metrics of the variation of the upper and lower horn height are presented in Table 2.

Table 2: Variation of upper ($\ell_{h_u}$) and lower ($\ell_{h_l}$) horn length for $k_s \in [0.1, 0.9]$ [mm].

| Cond. | $\ell_{h_u}$ | Predicted $\ell_{h_u}$ [mm] | | |
|---|---|---|---|---|
| No. | exp. † | mean | min | max |
| 3 | 36.3±2.6 | 30.5 | 15.9 | 37.7 |
| 7 | 16.0 | 16.4 | 10.4 | 20.0 |
| 9 | 21.6 | 18.1 | 9.9 | 23.2 |
| | $\ell_{h_l}$ | Predicted $\ell_{h_l}$ [mm] | | |
| No. | exp. | mean | min | max |
| 3 | 22.7±2.8 | 14.6 | 12.5 | 17.8 |
| 7 | 15.7 | 16.5 | 10.7 | 18.6 |
| 9 | 25.1 | 19.8 | 11.3 | 24.6 |

† [Mean ± std]. For Cond. 7 and 9 not enough repeated experiments.

Table 3: Variation of aerodynamic efficiency loss for $k_s \in [0.1, 0.9]$ [mm] based on clean airfoil.
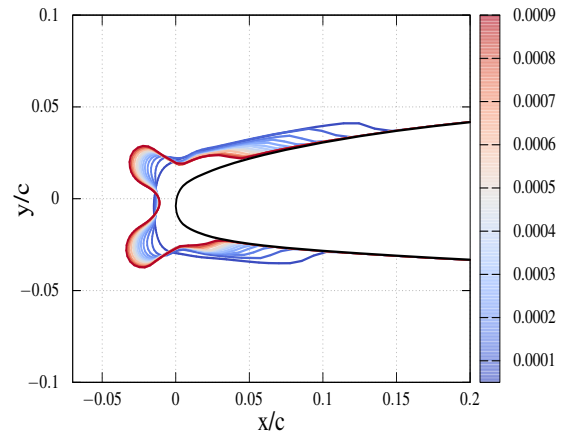
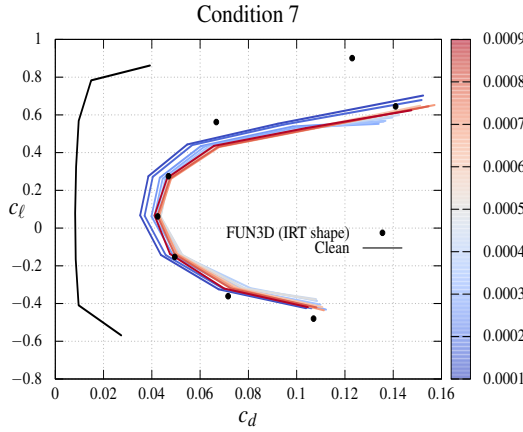| Cond. | $\left(\frac{c_l}{c_d}\right)_{max}$ | Predicted $\Delta\left(\frac{c_l}{c_d}\right)_{max}$ | | |
|---|---|---|---|---|
| No. | clean | mean | min | max |
| 3 | 71.6 | -61.0 | -52.9 | -63.5 |
| 7 | 58.6 | -51.7 | -50.5 | -52.3 |
| 9 | 74.4 | -62.8 | -55.2 | -64.3 |
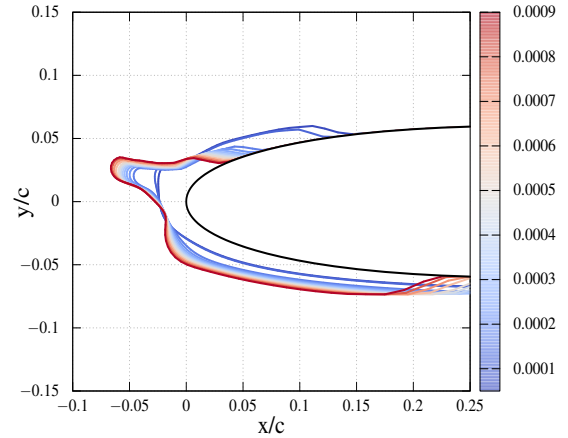


(a) Condition 3
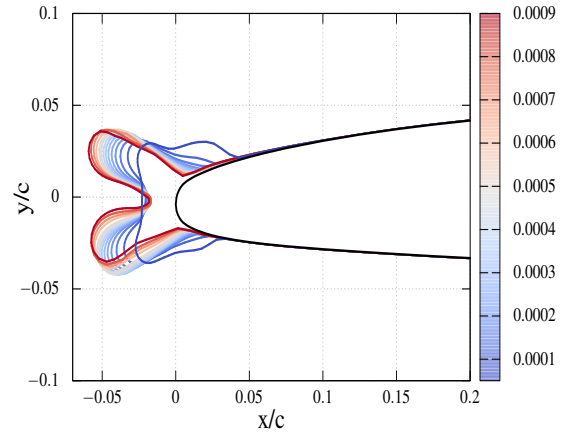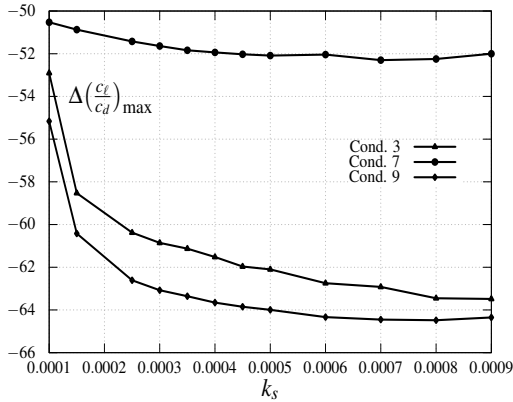


(b) Condition 7



(c) Condition 9

Figure 3: Variation of ice-shape prediction according to equivalent sand-grain roughness $k_s$ (shown in colormap).

(a)



(b)

Figure 4: Polar curves corresponding to ice shapes of Figure 1 for different equivalent sand-grain roughness $k_s$ (shown in colormap) using NSCODE-ICE.

## 4.2 Sensitivity on APD

In the previous section it was observed that the predicted ice shape depends considerably on the selected value of $k_s$. Therefore, the resulting prediction of APD, for the predicted ice shapes of Section 4.1, is also expected to vary accordingly. In this section, the variation of aerodynamic coefficients i.e. $c_d$ and $c_l$ with respect to the change in the input value of $k_s$ is investigated, and a quantification of the aerodynamic performance loss (drop in $\Delta(c_l/c_d)_{\max}$) is provided for angles of attack $\alpha \in [-6, 8]$ deg and $k_s \in [0.1, 0.9]$ mm. The polar shown in Figure 4a reflects on the sensitivity of $c_l$ and $c_d$ with respect to $k_s$. It is observed that for Condition 7 the performance loss due to icing (comparing to the clean shape) is significant, but not sensitive to the value of $k_s$, at least for the selected value interval. This is also shown in Figure 4b, where the

loss in maximum aerodynamic efficiency $\Delta(c_l/c_d)_{\max}$ can be seen to vary little in this $k_s$ range. In general, Figure 4b shows that as $k_s$ increases, performance loss will increase, mainly due to the glaze horn formation, that is related to higher rates of heat transfer. It is also observed that for Conditions 3 and 9 and for $k_s \in [0.1, 0.5]$ mm, the prediction of APD is much more sensitive than for values of $k_s \in [0.6, 0.9]$ mm. In the interval $k_s \in [0.1, 0.5]$ mm, and particularly for lower values in this interval, there is a strong sensitivity of the prediction to $k_s$. This is attributed to the fact that, at this point, there is a transition of the ice shape, from streamlined glaze ice shape (less detrimental to APD) to glaze ice shape with protruding horns (Figure 3a, Figure 3c). In contrast, for $k_s \in [0.6, 0.9]$, and for the larger values in this interval, the sensitivity is almost zero for all of the three conditions. The prediction of the loss in maximum aerodynamic efficiency $\Delta(c_l/c_d)_{\max}$, which is important for aircraft climb performance, is summed up in Table 3, quantifying the aforementioned trends. Thus, from these observations it can be deduced that the predictive confidence of APD can be considerably hindered by uncertainties in $k_s$ correlations [4], especially when the combination of icing conditions and heat transfer prediction is close to the threshold of horn formation.

## 5 CONCLUSIONS

For the current study, the NASA/ONERA benchmark was initially performed for the prediction of both ice shape and aerodynamic performance degradation. This was considered important to validate NSCODE-ICE for the given, extreme, atmospheric icing conditions producing glaze ice shapes. Having validated the icing simulation code, demonstrating that it can provide predictions of comparable quality comparing to LEWICE and IGLOO2D, the sensitivity study follows for values of $k_s$ ranging from 0.1 to 0.9mm. In Section 4.1, variations of the ice shape prediction for different values of $k_s$ were quantified by monitoring specific metrics of the geometry of an ice shape. The predicted ice shapes were subsequently used to predict the aerodynamic performance loss. The study shows that, for the current interval of $k_s$ values, two zones can be distinguished: i) for lower values of $k_s$ there is a high sensitivity of APD to $k_s$ which is connected to the start of glaze horn formation and a higher rate of increase of the ice horns and ii) for higher values of $k_s$ the sensitivity approaches zero as the rate of increase of ice horns drops. Considering that the sensitivity can vary considerably, at least in the interval under study, the uncertainties introduced by using the existing $k_s$ correlations can be significant.

Table 4: Ice shape metrics for the NASA/ONERA glaze ice benchmark. [28]

| Cond. No. | Ice Area $10^{-3}\ m^2$ | | | | | | | Run No. |
|---|---|---|---|---|---|---|---|---|
| | LEWICE | % Err | NSCODE-ICE | % Err | IGL2DMS[†] | % Err | EXP. | |
| 3 | 1.6067 | 0.8 | 2.1156 | 32.7 | 2.3650 | 48.3 | 1.5943 | AE1005936 |
| 7 | 0.3049 | 60.1 | 0.2125 | 11.6 | 0.3905 | 105.1 | 0.1904 | HC1072436 |
| 9 | 0.8647 | 8.8 | 0.8872 | 11.6 | 1.1386 | 43.3 | 0.7948 | HE1078536 |
| Cond. No. | Horn Height upper/lower, *mm* | | | | | | | Run No. |
| 3 | 25.8/14.7 | 25.0/33.8 | 29.2/- | 15.1/- | 33.2/15.9 | 3.5/28.4 | 34.4/22.2 | AE1005936 |
| 7 | 14.5/15.0 | 10.5/7.4 | 14.5/14.7 | 10.5/9.2 | 21.9/23.9 | 35.2/47.5 | 16.2/16.2 | HC1072436 |
| 9 | 17.5/19.5 | 19.0/22.3 | 15.9/17.9 | 26.4/28.7 | 21.6/24.7 | 0.0/1.6 | 21.6/25.1 | HE1078536 |
| Cond. No. | Horn Angle upper/lower, deg. | | | | | | | Run No. |
| 3 | 28/- | 33.3/- | 19.5/- | 53.6/- | 31/47 | 26.2/42.0 | 42/81 | AE1005936 |
| 7 | 49/44 | 88.5/100.0 | 28.2/25.5 | 8.5/15.9 | 40/40 | 53.8/81.8 | 26/22 | HC1072436 |
| 9 | 54/54 | 12.5/12.5 | 40.3/35.7 | 16.0/25.6 | 44/44 | 8.3/8.3 | 48/48 | HE1078536 |

[†] IGLOO2D Multistep

The quantification and the propagation of uncertainties within the icing simulation code was out of the scope of the current study as it was considered very complicated for this multiphysical problem. Instead, in order to reduce uncertainties related to roughness effects on heat transfer, a new comprehensive model proposed by Aupoix [1] is being implemented in NSCODE-ICE that takes into account the equivalent-sand grain roughness height $k_s$ as well as the true roughness height $k$ and the corrected wet surface $S_{corr}$. Despite the fact that the computation of the new added parameters is not a trivial task, they directly express heat-transfer related physics and permit the fine-tuning of convective heat transfer. There is a requirement to develop correlations for $k_s$, $k$ and $S_{corr}$ which will reduce uncertainty, by being calibrated using the NASA/ONERA benchmark.

## REFERENCES

[1] B. Aupoix. Improved heat transfer predictions on rough surfaces. *International Journal of Heat and Fluid Flow*, 56:160–171, 2015.

[2] B. Aupoix and P. R. Spalart. Extensions of the Spalart-Allmaras turbulence model to account for wall roughness. *International Journal of Heat and Fluid Flow*, 24:454–462, 2003.

[3] H. Beaugendre and F. Morency. FENSAP-ICE: Roughness Effects on Ice Accretion Prediction. In *41st Aerospace Sciences Meeting and Exhibit*, Aerospace Sciences Meetings. American Institute of Aeronautics and Astronautics, jan 2003.

[4] C. Bhatt and S. McClain. Assessment of uncertainty in equivalent sand-grain roughness methods. In *ASME International Mechanical Engineering Congress and Exposition, Volume 8: Heat Transfer, Fluid Flows, and Thermal Systems, Parts A and B*, pages 719–728, 2007.

[5] J. P. Bons. St and $c_f$ Augmentation for Real Turbine Roughness With Elevated Freestream Turbulence. *Journal of Turbomachinery*, 124(4):632, 2002.

[6] J. P. Bons, S. T. McClain, Z. J. Wang, X. Chi, and T. I. Shih. A Comparison of Approximate Versus

Exact Geometrical Representations of Roughness for CFD Calculations of $c_f$ and St. *Journal of Turbomachinery*, 130(2):021024, 2008.

[7] S. Bourgault-Cote, J. Docampo-Sánchez, and E. Laurendeau. Multi-Layer Ice Accretion Simulations Using a Level-Set Method With B-Spline Representation. In *2018 AIAA Aerospace Sciences Meeting*, AIAA SciTech Forum. jan 2018.

[8] S. Bourgault-Côté and E. Laurendeau. Development of a morphogenetic ice accretion solver using overset grids. In *CFD Society of Canada 24th Annual Conference*. CFDSC, June 2016.

[9] H. Coleman, B. Hodge, and R. Taylor. A Re-Evaluation of Schlichting's Surface Roughness Experiment. *ASME. J. Fluids Eng.*, 106(1):60–65, 1984.

[10] H. W. Coleman, B. K. Hodge, and R. P. Taylor. Generalized Roughness Effects on Turbulent Boundary Layer Heat Transfer. Technical report, Mississippi State University, ADA141943, 1983.

[11] R. Dirling. A method for computing rough wall heat transfer rates on reentry nose tips. *AIAA paper no. 73-763*, 1973.

[12] D. Hanson and M. Kinzel. An Improved CFD Approach for Ice-Accretion Prediction Using the Discrete Element Roughness Method. In *ASME 2017 Fluids Engineering Division Summer Meeting*, Waikoloa, 2017.

[13] K. Hasanzadeh, E. Laurendeau, and I. Paraschivoiu. Quasi-Steady Convergence of Multistep Navier-Stokes Icing Simulations. *Journal of Aircraft*, 50(4):1261–1274, june 2013.

[14] K. Hasanzadeh, E. Laurendeau, and I. Paraschivoiu. Grid-Generation Algorithms for Complex Glaze-Ice Shapes Reynolds-Averaged Navier-Stokes Simulations. *AIAA Journal*, 54(3):847–860, 2016.

[15] R. K. Jeck. Icing Design Envelopes (14 CFR Parts 25 and 29 , Appendix C) Converted to a Distance-Based Format. Technical Report April, Federal Aviation Administration, 2002.

[16] W. Kays and M. Crawford. *Convective Heat and Mass Transfer*. McGraw-Hill, New-York, 3 edition, 1993.

[17] P. Lavoie, S. Bourgault-Côté, and E. Laurendeau. Numerical algorithms for infinite swept wing ice accretion. *Computers Fluids*, 161:189 – 198, 2018.

[18] P. Lavoie, D. Pena, Y. Hoarau, and E. Laurendeau. Comparison of thermodynamic models for ice accretion on airfoils. *International Journal of Numerical Methods for Heat & Fluid Flow*, April 2018.

[19] S. T. McClain, B. K. Hodge, and J. P. Bons. Predicting Skin Friction and Heat Transfer for Turbulent Flow Over Real Gas Turbine Surface Roughness Using the Discrete Element Method. *Journal of Turbomachinery*, 126(2):259, 2004.

[20] E. Montreuil, A. Chazottes, D. Guffond, A. Murrone, F. Caminade, and S. Catris. ECLIPPS: 1. Three-Dimensional CFD Prediction of the Ice Accretion. In *1st AIAA Atmospheric and Space Environments Conference*. American Institute of Aeronautics and Astronautics, jun 2009.

[21] J. Nikuradse. Laws of flow in rough pipes. *VDI Forschungsheft*, page 361, 1933.

[22] A. Pigeon, A. T. Levesque, and E. Laurendeau. Two-dimensional Navier-Stokes flow solver developments at Ecole Polytechnique de Montreal. In *CFD Society of Canada 22nd Annual Conference, CFDSC*, 2014.

[23] H. Schlichting. Experimental investigation of the problem of surface roughness. Technical report, Ing.-Arch 7(1), NACA, 1936. TM–823.

[24] J. Shin, B. Berkowitz, H. Chen, and T. Cebeci. Prediction of ice shapes and their effect on airfoil performance. Technical report, NASA, 1991. TM–103701.

[25] A. Sigal and J. Danberg. New correlation of roughness density effect on the turbulent boundary layer. *AIAA Journal*, 28(3):554–556, 1990.

[26] R. C. Swanson and E. Turkel. On central-difference and upwind schemes. *Journal of Computational Physics*, 101(2):292–306, 1992.

[27] K. Szilder and E. P. Lozowski. Novel two-dimensional modeling approach for aircraft icing. *Journal of Aircraft*, 41(4):854–861, 2004.

[28] P. Trontin, A. Kontogiannis, G. Blanchard, and P. Villedieu. Description and assessment of the new ONERA 2D icing suite IGLOO2D. *9th AIAA Atmospheric and Space Environments Conference, Denver*, 2017.

[29] T. G. Trucano. Prediction and uncertainty in computational modeling of complex phenomena: A whitepaper. Technical report, Sandia National Laboratories, SAND98-2776.

[30] W. Wright. User's manual for lewice version 3.2. Technical report, NASA Glenn Research Center, NASA/CR-2008-214255, 2008.

[31] W. B. Wright. A Revised Validation Process for Ice Accretion Codes. *9th AIAA Atmospheric and Space Environments Conference, Denver*, 2017.

[32] C. Zhu, B. Fu, Z. Sun, and C. Zhu. 3D Ice Accretion Simulation for Complex Configuration Basing on Improved Messinger Model. *International Journal of Modern Physics: Conference Series*, 19:341–350, 2012.